10.18686/frim.v2i5.4528

A Novel Nanocatalyst for Combined Chemodynamic and Starvation Therapy in Cancer Treatment

Yingying Yang[1], Jinrong Situ[1], Hongzhang Yan[1], Lingle Zhang[1], Yingsheng Cheng[2,*]

1. Shanghai Ocean University, Shanghai, 201306

2. Shanghai Sixth People's Hospital, Shanghai, 201306

Abstract: Cancer remains a significant challenge due to the limitations and side effects of tra- ditional treatments. Novel minimally invasive therapies are essential to enhance patient outcomes. This study introduces MIL-101(Fe)@MnO_2 @Gox/HA, a nanocatalyst that com- bines glucose oxidase and manganese dioxide in an iron-based metal-organic framework (MOF) coated with hyaluronic acid. This nanoplatform demonstrates strong water affin- ity, tumor targeting, and durability. MIL-101(Fe)@MnO_2 @Gox/HA presents a promis- ing anti-cancer strategy, warranting further investigation to enhance tumor targeting and treatment efficacy.

Keywords: Nanocatalyst; Chemodynamic Therapy; Starvation Therapy; Cancer Treatment

1. Introduction

Cancer continues to be a major threat to human health and survival[1]. Tra- ditional treatments such as surgery, chemotherapy, and radiation have not signifi- cantly improved patients' quality of life or survival rates. Chemodynamic therapy (CDT) is an innovative and minimally invasive therapeutic strategy[2]. CDT kills tumor cells through Fenton reactions with H_2O_2 and strong catalysts, leveraging the high levels of H_2O_2 in the tumor microenvironment (TME). ROS, especially hydroxyl radicals (·OH), can cause oxidative damage to DNA, lipids, and proteins, leading to cell death [3]. Metal-organic frameworks (MOFs), which are made up of metal ions and organic ligands connected by coordination bonds, area new form of porous hybrid nanomaterial exploited in CDT. Starvation treatment (ST) is a novel method based on glucose restriction that slows tumor development by re- stricting the flow of blood, vital nutrients, and oxygen[4]. Glucose oxidase (Gox), an endogenous oxidoreductase, is a good alternative since it consumes oxygen and D-glucose, hence depleting glucose[5]. Clearly, the combination of CDT and ST has received a lot of interest in leveraging biocatalysts to consume glucose and cre- ate H_2O_2. This study suggests a therapeutic approach that is simple, regulated, repeatable, and cost-effective for clinical applications.

2. Materials and Methods

2.1 Materials

Aladdin Biochemical Technology Co., Ltd. supplied 99 percent potassium permanganate (KMnO4) and 17, 500 molecular weight polypropylene salt. MIL- 101 (Fe) nanoparticles and glucose oxidase (activity 10 KU) were purchased from Beijing Xi'an Ruixi Biotechnology Co., Ltd. Ron Chemical Reagents supplied the fluorescent dye Rhodamine B (molecular weight 479.01) and dimethyl sulfoxide (99.7%). All cell culture products were supplied by GIBCO (Grand Island, NY, USA). Nanjing Kaiji Biological Technology Co., Ltd. offered the Cell Counting Kit-8 (CCK-8), and the Annexin V-FITC/PI apoptosis detection kit.

2.2 Preparation of MIL-101(Fe)@MnO_2 @Gox/HA nanoplatforms

MIL-101(Fe)@MnO_2 nanoparticles were synthesized utilizing a slightly mod- ified technique from an earlier work. 10 mg of MIL-101-(Fe) was added to 10 mL of deionized water and agitated for 30 minutes, followed by the addition of 200 μL of potassium permanganate (10 mg/mL) and 200 μL of polyallylamine hydrochloride (23.6 mg/mL). Then, 6 mL of Gox (5 mg/mL), 3 mL of EDC (20 mM), 3 mL of NHS (20 mM) and 10 mL of MM solution (1 mg/mL) were added.

2.3 Characterization

The size and form of the nanoparticles were measured using a transmission electron microscope (TEM, JEM-2100F, Japan). The nanoparticles were analyzed using a Zetasizer Nano ZS instrument from Shanghai. We measured dynamic light scattering and investigated the zeta potential of the nanoparticles. The UV-Vis absorption spectra of nanoparticles solution were acquired using a UV- Vis spectrophotometer (Lambda 950, USA) to qualitatively investigate MnO_2 and GOx. The samples'chemical structure and content were analyzed by using Fourier-

transform infrared spectroscopy (FT-IR) with a Nicolet 6700 instrument from the USA.

2.4 Cell culture

In this investigation, the human gastric cancer MGC-803 cell line was employed in vitro assays and procured from the American Type Culture Collection (ATCC). Cells were grown in DMEM with 10%(v/v) fetal bovine serum (FBS) and 1% penicillin/streptomycin and maintained in a humidified incubator with 5% CO_2 at 37 ℃ .

2.5 Cell proliferation assessment

The CCK-8 test was performed to examine the cytotoxic effects of MIL-101(Fe), MMG, and MMGH in vitro. Human gastric cancer MGC-803 cells were planted in a 96-well plate at a density of 1×10^4 cells per well and incubated for 24 hours. Next, different volumes of Gox solution were added. After 6 hours of incubation, the cells were washed three times with PBS before being incubated again with fresh DMEM medium. To each well, 100 μL of medium containing 10 μL CCK-8 was added to the cells. After an hour of incubation, the absorbance at 450 nm was measured.

2.6 Cellular uptake assay

Fluorescence microscopy and flow cytometry were utilized to visualize and measure the cellular uptake and distribution of MMG and MMGH in MGC-803 cells. The cells were treated with MMG and MMGH at the same Gox dosage of 0.1 μg/ml for 1 hour and 6 hours, respectively. Following PBS washing, the cells were stained with 4', 6-diamidino-2-phenylindole (DAPI) for nuclear staining and Rhodamine-B for Gox labeling. After complete cell washing, the fluorescence of the cells was captured using an inverted fluorescent microscope. Flow cytome- try studies were performed to determine MMG and MMGH's cellular absorption efficiency.

2.7 Statistical analysis

Statistical comparisons across various groups were undertaken using a student's t-test. *$p<0.05$ was deemed statistically significant. **$p<0.01$ and ***$p<0.001$ were judged extremely significant.

3. Results and discussion

3.1 Preparation and characterization of MMGH

The produced MIL-101(Fe) material was studied by transmission electron mi- croscopy (TEM) to disclose the morphology of MIL-101-(Fe), MM, MMG, and MMGH nanoparticles at different scales(Figs. 1A to 1D). MIL-101(Fe) nanoparti- cles have ahomogeneous polyhedral structure with an average diameter of 100 nm. The resulting products meet expectations, with an average diameter of 200 nm. Compared to MIL-101(Fe), the UV-Vis spectra of MIL-101(Fe)@MnO_2 display broad and considerable light absorption in the range of 300 to 500 nm (Fig. 1E), corresponding to the normal absorbance peaks of MnO_2, suggesting the synthesis

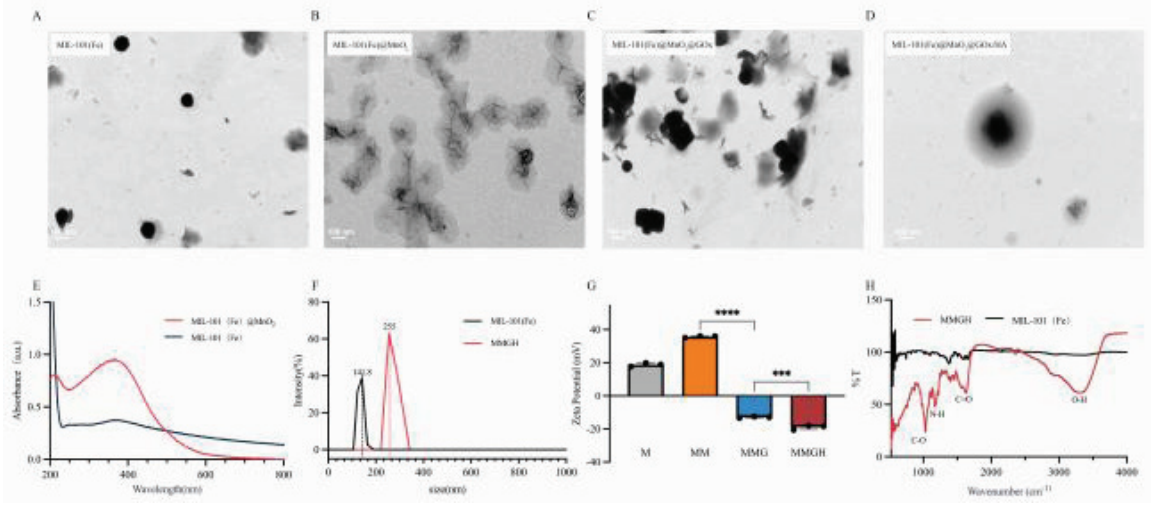

Figure 1: Characterization of MMGH nanoparticles.

TEM images of (A) MIl-101(Fe), (B) MM, (C) MMG and (D) MMGH. (E) UV-vis spectra of MIL-101(Fe) and MM. (F) Hydrodynamic diameter of MIL-101(Fe) and MMGH. (G) Zeta Potential of MIL-101(Fe), MM, MMG and MMGH. (H) FTIR of MIL-101(Fe) and MMGH.

Of MnO_2 inside MIL-101(Fe). Dynamic light scattering was employed to determine the average hydrodynamic diameters of MIL-101-(Fe) and MMGH, which were about 141.8 and 255 nm, respectively (Fig. 1F). The negatively charged GOx and HA neutralize some of MIL-101(Fe)@MnO_2 's positive charge. Positively charged molecules are more easily absorbed by cells across the cell membrane, which is useful

for producing more favorable therapeutic effects both in vivo and in vitro (Fig. 1G). The FTIR tests revealed separate absorption peaks for GOx and HA (Fig. 1H). The C=O stretching vibration peaks were discovered between 1700 and 1500 cm-1, whereas the ·OH stretching vibration peaks were detected be- tween 3600 and 3200 cm-1. Furthermore, the reduction in the ·OH absorption peak in MMGH indicates that GOx and HA were successfully loaded onto MM.

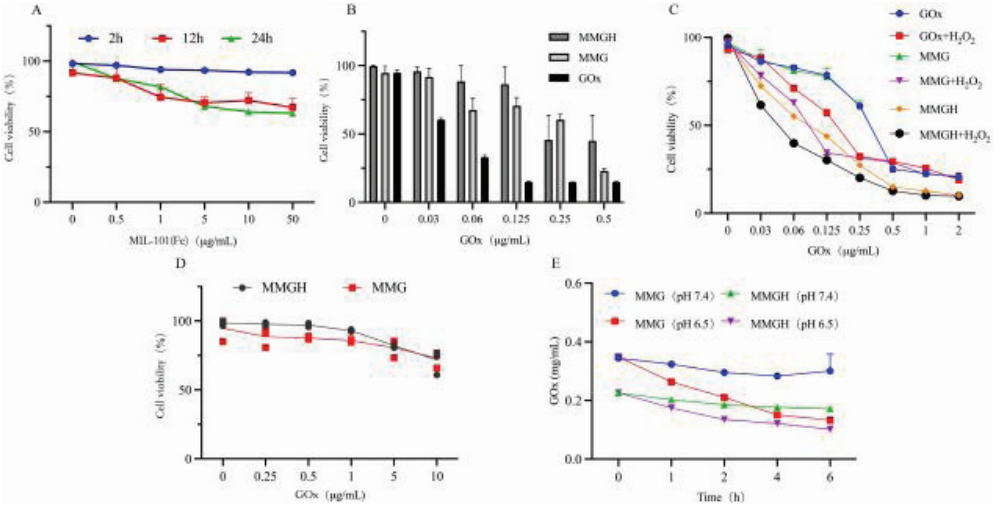

Figure 2: Cell proliferation and drug release.

(A) The viability of MGC-803 cells after treatment with different concentrations of MIL-101 (Fe) at different times (n=3). (B) The viability of MGC-803 cells after treatment with GOx, MMG, and MMGH over time (n=3). (C) The viability of MGC-803 cells after treatment with different concentrations of GOx, MMG, and MMGH (n=3). (D) The viability of GES-1 cells after treatment with different concentrations of MMG and MMGH (n=3). (E) GOx release of MMG and MMGH at different pH.

3.2 Cellular toxicity of MMGH

Cell cytotoxicity testing was done on MGC-803 tumor cells. MIL-101(Fe) demonstrated modest cytotoxicity (Fig. 2A), which was augmented by the addi- tion of H_2O_2 to boost ·OH production, hence amplifying this toxicity. Meanwhile, MM demonstrated concentration-dependent cell death, likely owing to the reac- tion of MnO_2 creating O_2, which encouraged the Fenton reaction and subsequent ·OH production. Both GOx and MMG demonstrate significant rates of glucose consumption, hence competing with tumor cells for glucose(Fig. 2B). Therefore, the strong lethal impact of GOx on MGC-803 cells may be attributed to glucose deprivation. When the concentration of GOx rose to 0.125 μg/mL, cell viability was suppressed by almost 70%, while GOx at 0.25 μg/mL demonstrated consid- erable cytotoxicity in the nanostructure. Hence, 0.25 μg/mL was selected as the

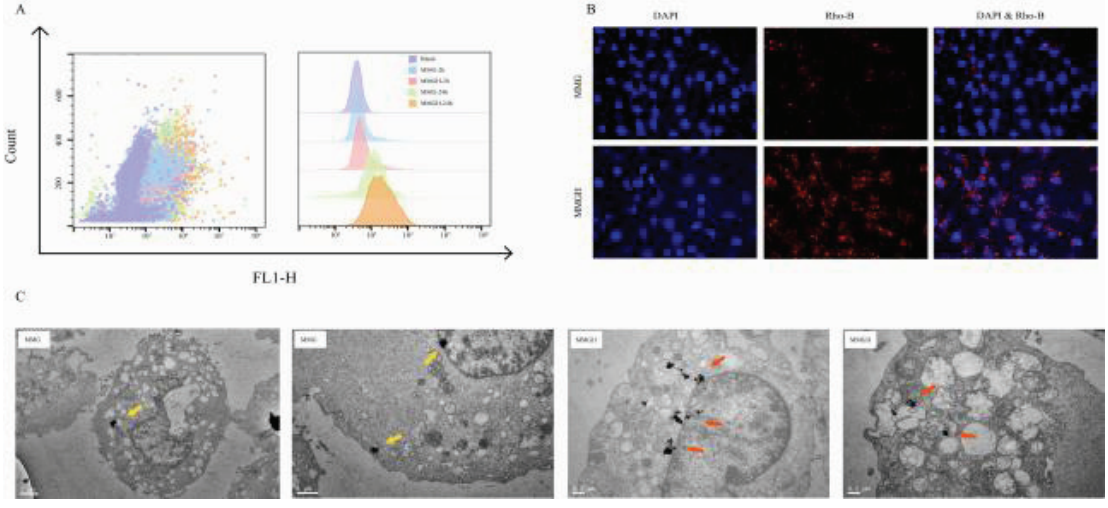

Figure 3: Cell uptake and distribution.

(A) Cell distribution analysis using flow cytometry under response conditions. (B) Fluorescence image of MGC-803 cells after treatment with MMG or MMGH. (C) TEM images of MMG and MMGH internalized by MGC-803 cells.

Best dose of GOx for the following investigations. The capacity of MMG and MMGH to kill tumor cells is considerably increased by H_2O_2 (Fig. 2C). Higher H_2O_2 concentrations in the Fenton-like reaction are good for creating At pH 7.4, the release rate of GOx from MMGH was lower than that from MMG, likely due to the inhibition of GOx release by the HA coating(Fig. 2E). The HA coating would help to minimize its cytotoxicity in normal tissues even more.

3.3 Cellular uptake and distribution of MMGH

Fluorescence microscopy indicated that MMGH had greater cellular absorp-tion than MMG (Fig. 3A), which was validated by flow cytometry data (Fig. 3B). Transmission electron microscopy demonstrated that both MMGH and MMG could penetrate cells (Fig. 3C). It may be extrapolated that hyaluronic acid (HA) may readily identify and bind to CD44 receptors overexpressed on the surface of MGC-803 cells, suggesting that MMGH may have tumor cell targeting capabili- ties.

4. Conclusions

The study discusses a novel nano-catalyst developed by encapsulating Gox and MnO_2 within MIL-101(Fe) and then coating it with HA. This catalyst displays substantial hydrophilicity, tumor-targeting capabilities, and outstanding stability. The nano-amplifier demonstrates high tumor cell accumulation and enhances the levels of H^+, H_2O_2, and O_2 inside tumor cells. The increasing concentrations of H_2O_2 and O_2 promote CDT via Fenton-like activities and ST through enzyme- catalyzed reactions, respectively. Furthermore, increasing acidity increases the frequency of Fenton-like events and enzyme-catalyzed reactions, thereby strength- ening the therapeutic efficacy against CDT and ST. This nano-catalyst shows promise as an anticancer drug and deserves more research.

Conflits of interest

The authors declare no competing financial interest.

References

[1] Bhupender S. Chhikara and Keykavous Parang. “Global Cancer Statistics 2022: the trends projection analysis”. In: Chemical Biology Letters 10 (2023), pp. 451–451.

[2] F. Bray et al. “GLOBOCAN estimates of incidence and mortality worldwide for 36 cancers in 185 countries. CA Cancer J Clin”. In: (2018).

[3] Parris Kidd. “Astaxanthin, cell membrane nutrient with diverse clinical benefits and anti- aging potential”. In: Altern Med Rev 16.4 (2011), pp. 355–364.

[4] Shuangjiang Yu et al. “Advances in nanomedicine for cancer starvation therapy”. In: Ther- anostics 9.26 (2019). Publisher: Ivyspring International Publisher, p. 8026.

[5] Chunhui Wang et al. “Glucose Oxidase-Related Cancer Therapies”. en. In: Advanced Ther- apeutics 3.10 (Oct. 2020), p. 2000110. issn: 2366-3987, 2366-3987.